Supplement of The Cryosphere, 10, 2217–2239, 2016
http://www.the-cryosphere.net/10/2217/2016/
doi:10.5194/tc-10-2217-2016-supplement

The Cryosphere Open Access EGU

Supplement of

The impact of melt ponds on summertime microwave brightness temperatures and sea-ice concentrations

S. Kern et al.

Correspondence to: Stefan Kern (stefan.kern@uni-hamburg.de)

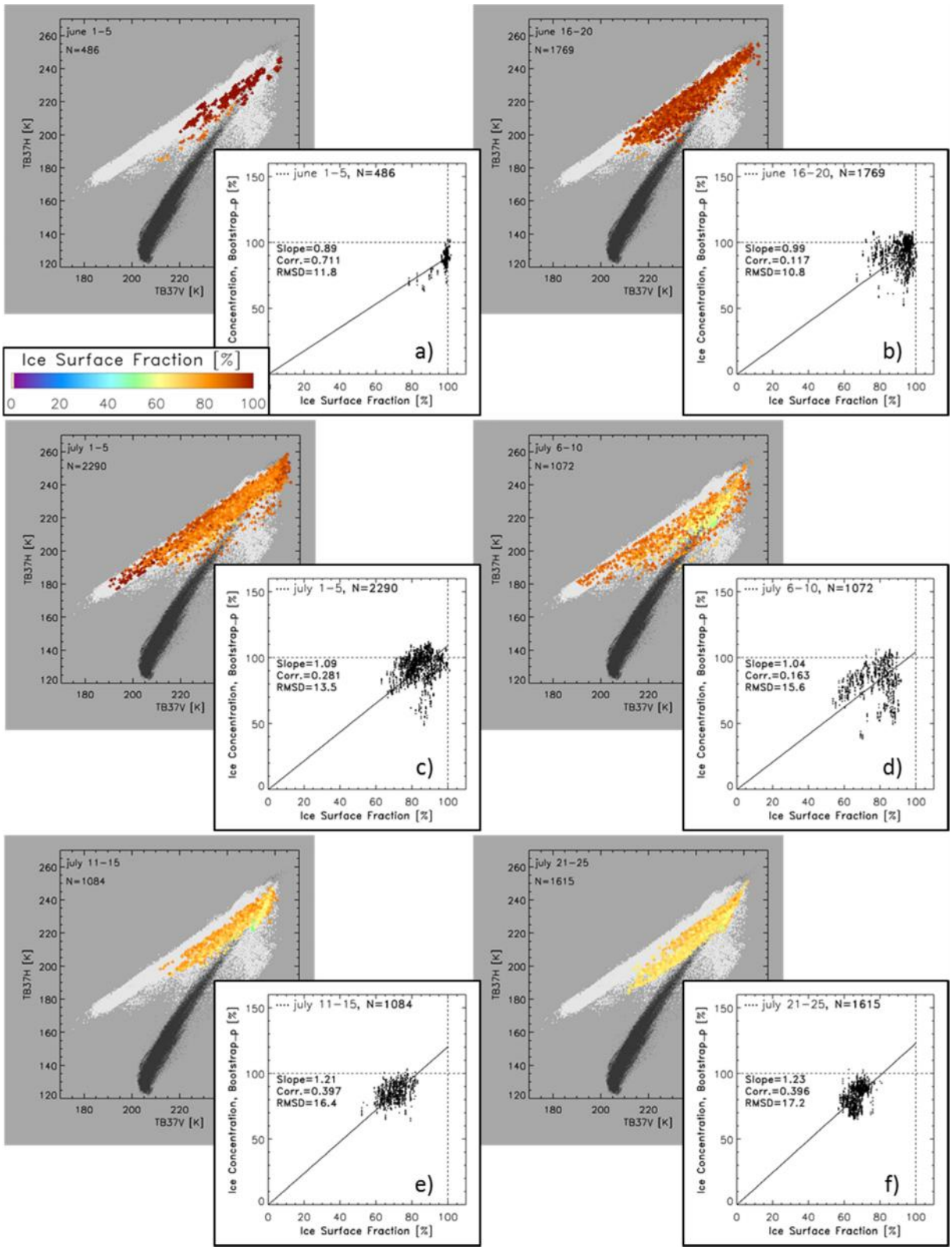

Figure S1. Background: 37 GHz AMSR-E brightness temperature at horizontal versus at vertical polarization, color-coded with the co-located MODIS ice-surface fraction for the same 6 selected pentads as in Figure 7 denoted in the upper left corner of each image together with the number N of data pairs. For white and black dots see Figure 6. Foreground: Same as in Figure 7 but for the Bootstrap_p algorithm.

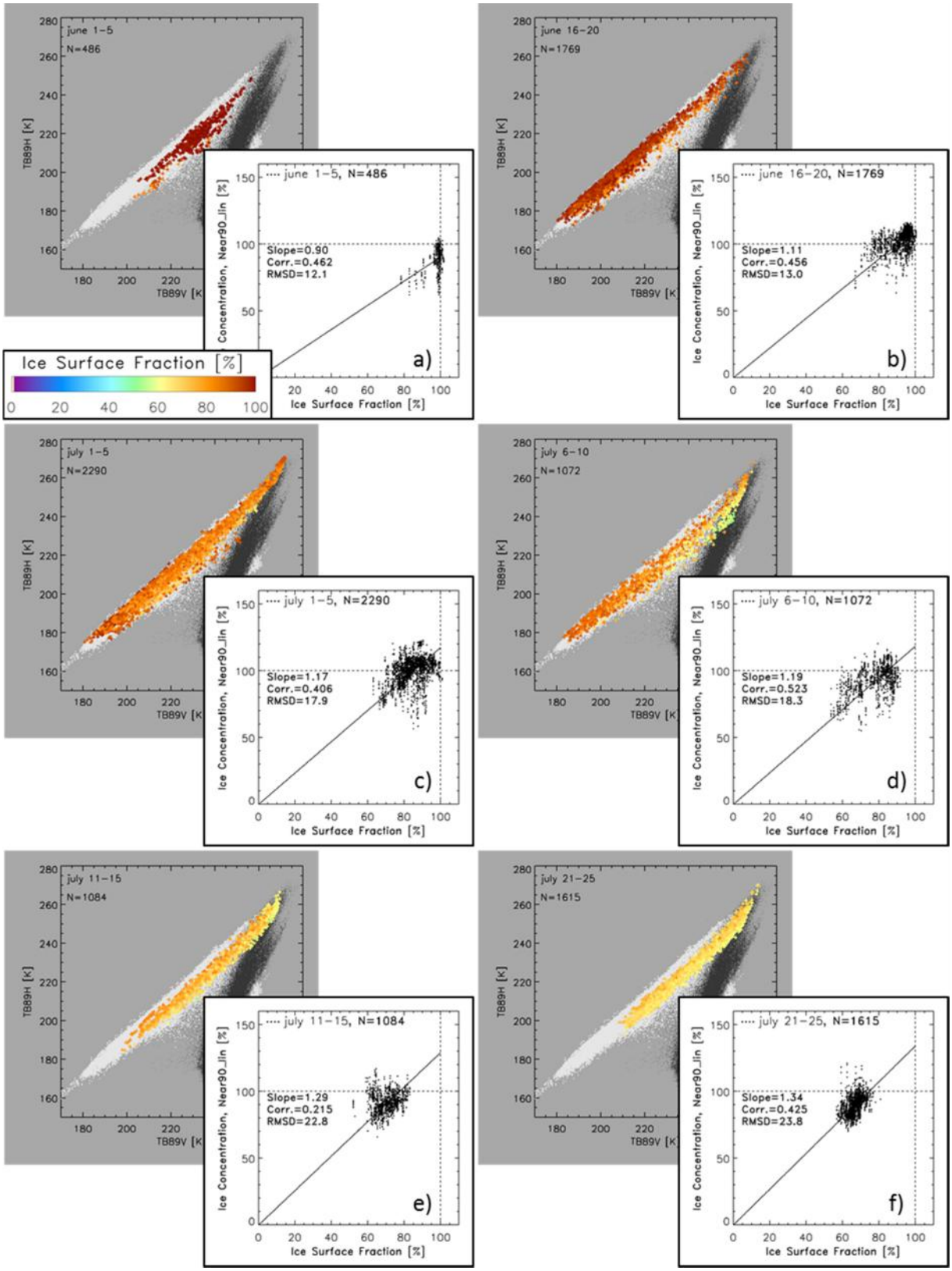

Figure S2. Background: 89 GHz AMSR-E brightness temperature at horizontal versus at vertical polarization, color-coded with the co-located MODIS ice-surface fraction for the same 6 selected pentads as in Figure 7 denoted in the upper left corner of each image together with the number N of data pairs. For white and black dots see Figure 6. Foreground: Same as in Figure 7 but for the Near90_lin algorithm.

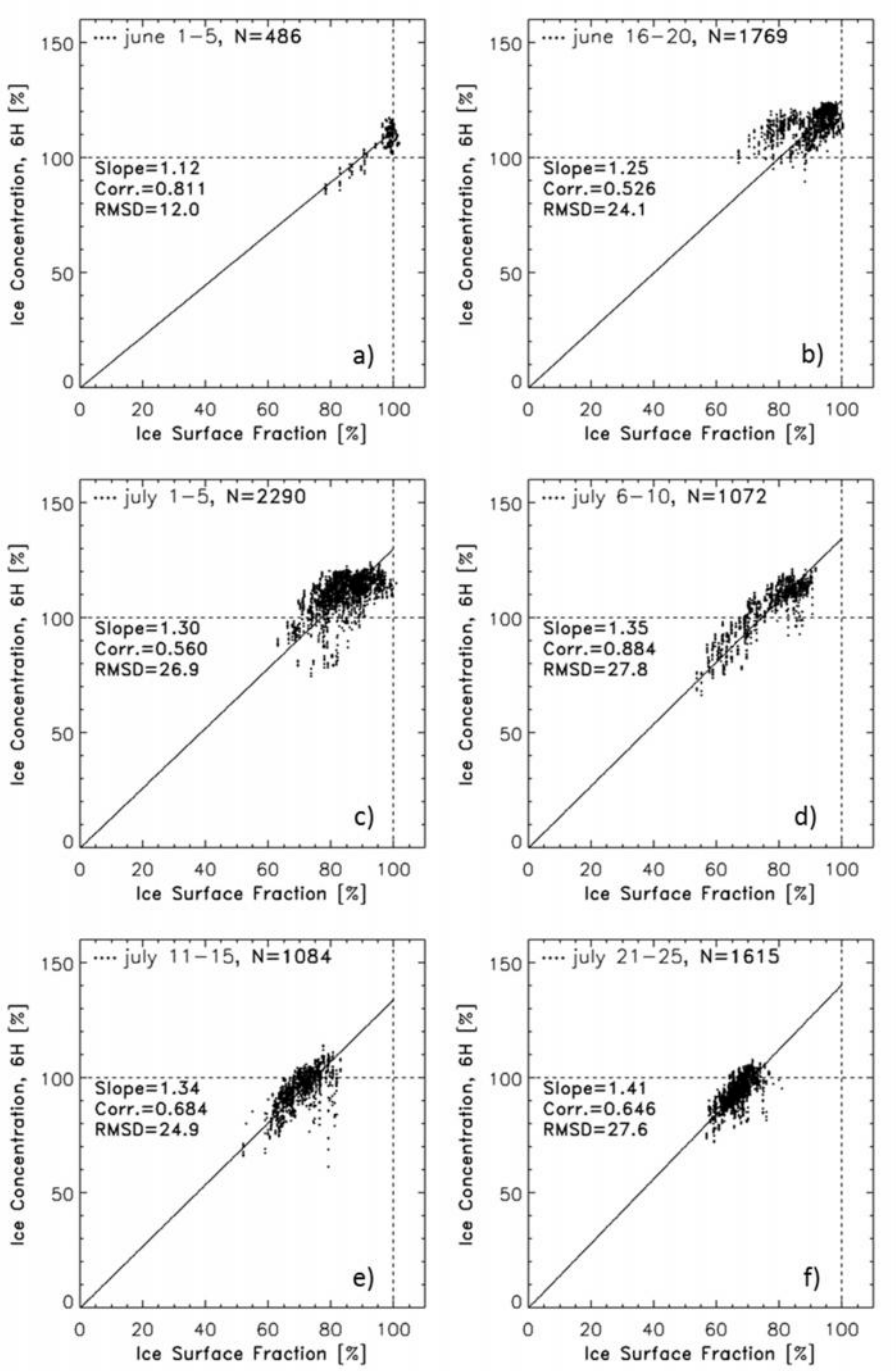

Figure S3. 6H algorithm sea-ice concentration versus MODIS ice-surface fraction for the same pentads together with the linear regression line forced through (0,0). The slope of this line is given together with the correlation between and the root mean squared difference (RMSD) of the two data sets in each image.

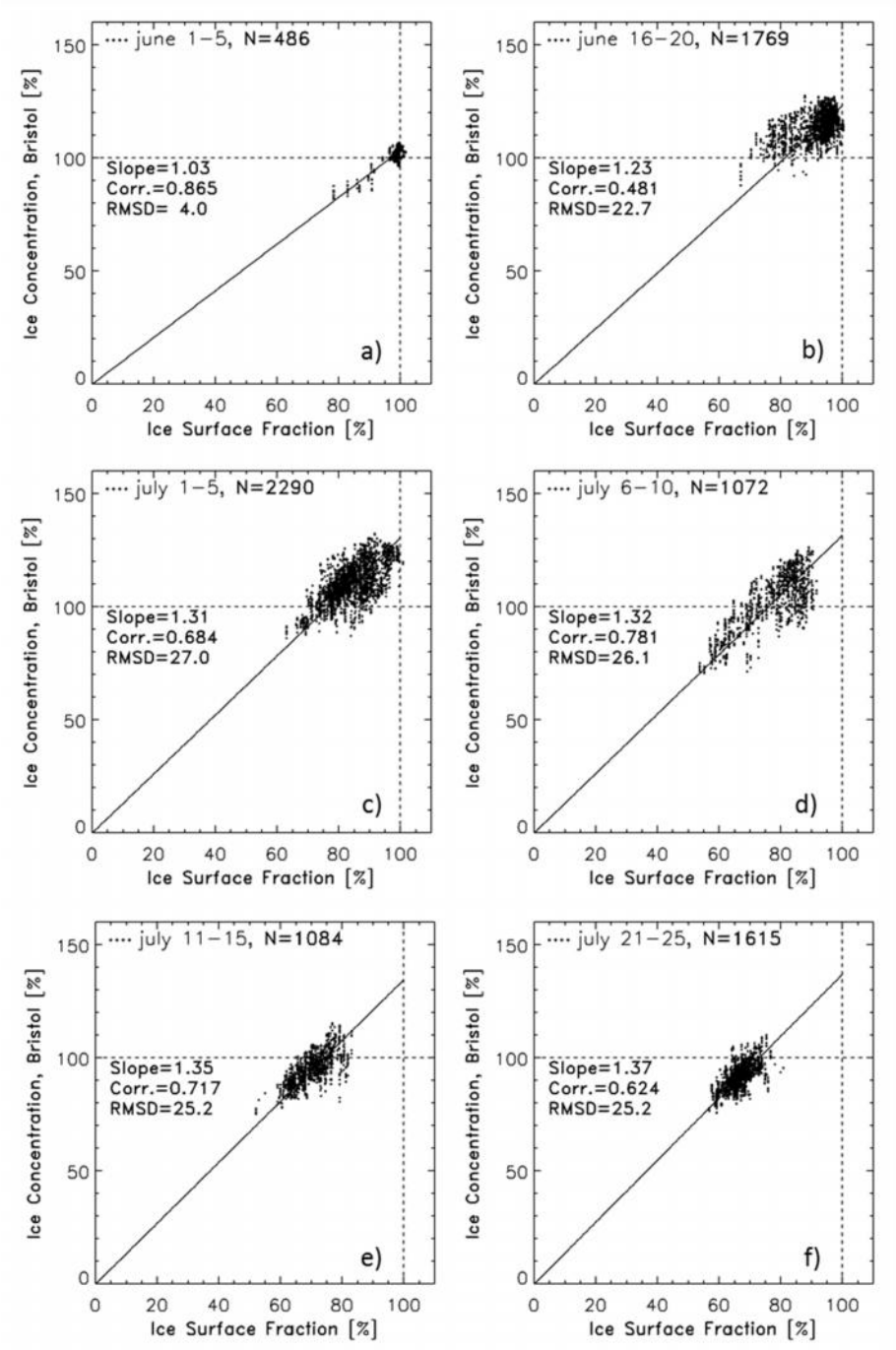

Figure S4. Bristol algorithm sea-ice concentration versus MODIS ice-surface fraction for the same pentads together with the linear regression line forced through (0,0). The slope of this line is given together with the correlation between and the root mean squared difference (RMSD) of the two data sets in each image.